Study on Properties of Gel Polymer Electrolytes Based on Ionic Liquid and Amine-Terminated Butadiene-Acrylonitrile Copolymer Chemically Crosslinked by Polyhedral Oligomeric Silsesquioxane

Ming Li, Wentan Ren, Yong Zhang, Yinxi Zhang

State Key Laboratory of Metal Matrix Composites, School of Chemistry and Chemical Engineering, Shanghai Jiao Tong University, Shanghai 200240, People's Republic of China

Received 24 November 2011; accepted 13 January 2012
DOI 10.1002/app.36906
Published online in Wiley Online Library (wileyonlinelibrary.com).

ABSTRACT: Based on amine-terminated butadiene-acrylonitrile copolymer chemically crosslinked by epoxycyclohexyl polyhedral oligomeric silsesquioxane (POSS), a novel gel polymer electrolyte (GPE) were prepared by introducing one ionic liquid and $LiClO_4$ into the polymer framework. Fourier transform infrared spectroscopy, field emission scanning electron microscopy, and X-ray diffraction analysis confirmed the interaction between the ionic liquid and $LiClO_4$, and this interaction contributes to dissolving $LiClO_4$ salt and increasing the ionic conductivity of GPE. Less content of POSS leads to higher ionic conductivities but lower gel content and modulus. The maximum ionic conductivity of 2.0×10^{-4} S cm^{-1} (30°C) was achieved and an Arrhenius-type relationship between ionic conductivities and temperatures could be detected over the investigated temperature range. The generated GPE exhibited good electrochemical stability to 4 V from cyclic voltammogram tests, which made this kind of GPE a promising candidate for rechargeable lithium batteries. © 2012 Wiley Periodicals, Inc. J Appl Polym Sci 000: 000–000, 2012

Key words: gel polymer electrolytes; polyhedral oligomeric silsesquioxane; ionic liquid; ionic conductivity

INTRODUCTION

Researchers have spent much effort on studying gel polymer electrolytes (GPEs) for lithium batteries since Feuillade[1] first reported them in 1975. GPEs are usually prepared by trapping lithium salt and organic solvent molecules into a crosslinked polymer network by soaking or blending. In GPE, lithium salt is mainly dissolved with the effect of organic solvent with polar groups. Owing to the higher mobility of lithium ions in the liquid phase of GPE structure,[2,3] the ionic conductivity of GPE is usually higher than liquid-free solid polymer electrolytes or similar to traditional liquid electrolytes. Besides, the safety problems of traditional liquid electrolyte batteries caused by leakage or instability upon cycling can be avoided in the application of GPE.[4] Based on these advantages, as the intermediate between traditional liquid electrolytes and liquid-free solid polymer electrolytes,[5] GPEs are promising candidates for lithium batteries.[6,7]

Compared with physically crosslinked GPE, chemically crosslinked GPE with covalent junction points and irreversible gels often exhibit better mechanical properties and dimensional stability, and avoid solvent leakage at high temperatures.[8,9] Ring-opening addition reaction of amino group toward epoxy group provides a favorable way to form chemical network[10–14] because of mild reaction condition and convenience for control of crosslinking density. Unlike the free radical crosslinking reaction with the aid of an initiator,[15] the absence of initiator and small molecular products for the epoxy–amine reaction is helpful to avoid side reactions caused by residual chemicals. So far, several GPE on the basis of neat epoxy–amine networks have been reported such as diglycidyl ether of bisphenol A-branched poly(ethyleneimine),[16] and butanediol diglycidylether–polyetherdiamine.[4]

As potential alternatives to conventional organic solvents, room temperature ionic liquids (ILs) have attracted considerable interest.[17] Most of them exhibit outstanding thermal and chemical stability, good ionic conductivity (10^{-3}–10^{-2} S cm^{-1} at room temperature), nonvolatility, nonflammability, solubility with many compounds and in some case high electrochemical stability up to 6 V.[18] Recently, the combination of polymer and IL has been studied as GPE for the lithium batteries.[19–23]

Polyhedral oligomeric silsesquioxane (POSS) is nanosized inorganic–organic hybrid. The inorganic

Correspondence to: W. Ren (1958rwt@sjtu.edu.cn).

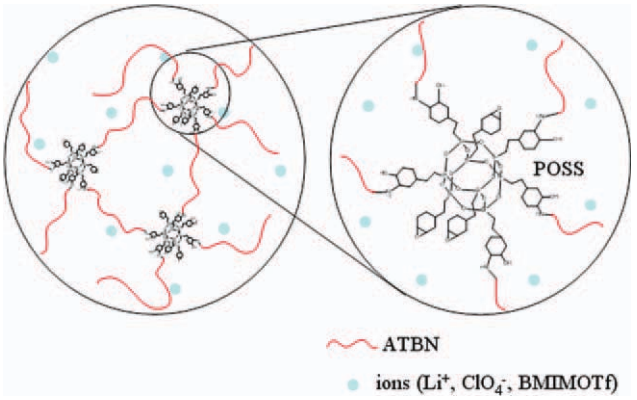

Figure 1 Schematic structure of GPE with POSS as crosslinking agent. [Color figure can be viewed in the online issue, which is available at wileyonlinelibrary.com.]

silica core can provide enhanced thermal stability and mechanical properties, and the organic branches with functional groups can provide accessibility of modification and reaction.[24–27] A class of oligo-oxyenthylene-functionalized POSS was developed as electrolytes for lithium batteries by Wunder.[28–30] Another solid polymer electrolyte based on crosslinkable methacryl-POSS was prepared with UV curing method by Park.[31] In this study, we prepared new GPE based on amine-terminated butadiene-acrylonitrile (ATBN) copolymer with epoxycyclohexyl POSS as crosslinking agent (Fig. 1).[32] The self-standing and homogenous GPE membranes were obtained by confining $LiClO_4$ and 1-butyl-3-methylimidazolium trifluoromethanesulfonate (BMIMOTf), a kind of IL, into the polymer framework by thermal curing. The prepared GPE was characterized by kinds of measurements and performed excellent ionic conductivity and good electrochemical properties.

EXPERIMENTAL

Materials

ATBN with acrylonitrile content of 18 wt % and amine equivalent weight of 900 g eq^{-1}. (Hycar® ATBN 1300X16) was purchased from Noveon, Cleveland, OH. Epoxycyclohexyl POSS (EP0408; $(C_8H_{13}O)_m(SiO_{1.5})_m$, $m = 8$, 10, 12; formula weight = 1772.73 g mol^{-1}) was purchased from Hybrid Plastics (Hattiesburg, MS). $LiClO_4$ (A.R., Sinopharm Chemical Reagent, China) and BMIMOTf (99%, Shanghai Cheng Jie Chemical, China) were vacuum dried for 24 h at 120°C, respectively. Tetrahydrofuran, (THF, Sinopharm Chemical Reagent, China) was distilled over sodium under dry nitrogen atmosphere prior to use. Methanol (A.R. Sinopharm Chemical Reagent, China) was used as received.

Preparation of GPE samples

ATBN was first dissolved in THF and precipitated in methanol for purification. The precipitated ATBN was washed with methanol for several times before vacuum drying at 50°C for 24 h. A solution of the purified ATBN, epoxycyclohexyl POSS, $LiClO_4$, and BMIMOTf in THF was stirred vigorously for 30 min and cast into Teflon® moulds. After the volatilization of THF, the precursors in moulds were cured at 100°C for 6 h to allow a crosslinking reaction. The resulting GPE membranes were self-standing and optically homogenous. The schematic structure of GPE is shown in Figure 1. The GPE samples used in this study were denoted as ATBN-x%POSS-y%$LiClO_4$-z%IL which means the contents of epoxycyclohexyl POSS, $LiClO_4$, and BMIMOTf were x, y, and z wt % to the weight of ATBN, respectively.

Characterization

The Fourier transform infrared spectroscopy (FTIR) measurements were conducted using a Perkin-Elmer Spectrum 100 spectrometer with a resolution of 1 cm^{-1} at room temperature in the wavenumber range of 4000–450 cm^{-1}. Morphology of the GPE specimens was studied by field emission scanning electron microscopy (FESEM; JSM-7401F JEOL, Japan). Images were taken from cryogenically fractured surfaces sputter-coated with gold. X-ray diffraction (XRD) measurements were carried out at room temperature on a D/MAX-2200/PC diffractometer (Rigaku, Tokyo, Japan), using the Cu Kα radiation at 40 kV/20 mA for 2θ values between 10 and 50 with a scanning speed of 4 min^{-1}. Dynamic mechanical analysis (DMA) was performed on a TA Q800 instrument using tensile mode with a fixed amplitude of 0.5% at 30°C. The storage modulus (G') and loss modulus (G'') were measured as a function of frequency within the range of 0.5–50 Hz. The gel content of GPE samples was measured to determine the extent of crosslinking by POSS. GPE samples were weighed before and after extraction by THF for 72 h in a Soxhlet extractor. The gel content can be calculated as the ratio of the left sample mass to the original sample mass.

GPE membranes were sandwiched between two stainless steel (SS) blocking electrodes to form a symmetrical SS/GPE/SS cell, and then ionic conductivity was measured by alternating current complex impedance analysis using Autolab PGSTA302 electrochemical test system in the frequency range form 1 MHz to 1 Hz under the signal amplitude of 10 mV. The stack SS/GPE/SS was stored in an oven for at least 30 min at each temperature before the impedance response was recorded. Autolab PGSTA302 electrochemical test system was also used to conduct

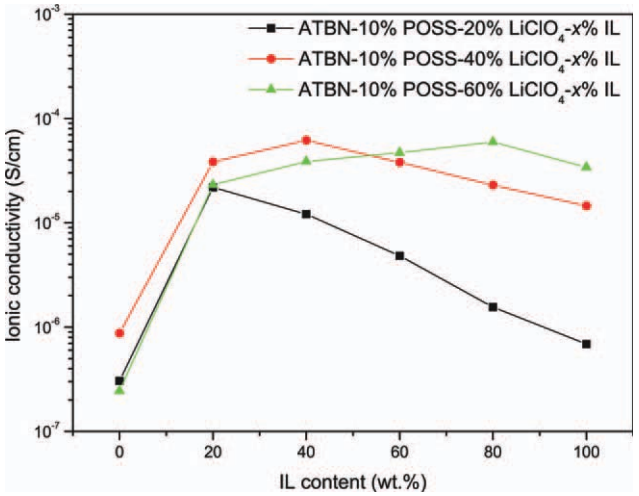

Figure 2 Ionic conductivity of GPE based on ATBN with different $LiClO_4$ and IL contents. [Color figure can be viewed in the online issue, which is available at wileyonlinelibrary.com.]

cyclic voltammogram (CV) measurement with a three-electrode cell, Al/GPE/Li, with aluminum as the blocking working electrode, lithium as both the counter and the reference electrode and the GPE membrane as the electrolyte. The cell was assembled and sealed in an argon-filled UNLAB glove box and was tested between −0.5 and 4.0 V at a constant scanning rate of 50 μV s^{-1} at 25°C.

RESULTS AND DISCUSSION

Ionic conductivity

Figure 2 shows the ionic conductivity of the prepared GPE at 25°C as a function of IL content. With POSS content set at 10 wt % and $LiClO_4$ content at 20, 40, and 60 wt %, the ionic conductivity of these three series of GPE shows the same trend with increasing IL content. Compared with the IL noninvolved samples, samples with 20 wt % IL exhibit much higher ionic conductivity. The ionic conductivity increases to a peak value at a certain content of IL for each system, 20 wt % IL for GPE with 20 wt % $LiClO_4$, 40 wt % IL for GPE with 40 wt % $LiClO_4$, and 80 wt % IL for GPE with 60 wt % $LiClO_4$. Further increasing IL content leads to a slight decrease of ionic conductivity, which might be caused by the dilution of lithium ion in the composites.

FTIR analysis

The characteristic peaks of IL show up in the spectra of GPE with 10 wt % POSS, 40 wt % $LiClO_4$, and different contents of IL, and become more and more apparent with increasing IL content [Fig. 3(a)], such as the peak at 1574 cm^{-1} corresponding to the stretching vibration of C=N in the imidazole ring,[33] the peaks at 1032 and 1167 cm^{-1} ascribed to C=F and S—O stretching vibration mode. However, the peak at 851 cm^{-1} corresponding to S—O bond in the spectrum of IL shifts to 845 cm^{-1} in the GPE spectra,[34] which might result from the change of S—O bond by the influence of lithium ions.

In addition, the absorption band around 1102 cm^{-1} corresponds to the asymmetric stretching vibration of free perchlorate anion.[35] The band separates into two or three adjacent peaks when ClO_4^- coordinated with Li^+ in monodentate or bidentate state, such as the three peaks at 1088, 1112, and 1144 cm^{-1} in the spectrum of $LiClO_4$, which indicate that the $LiClO_4$ mainly exists as complexes but not free ions. Similarly, three less evident peaks can be observed in the spectrum of ATBN-10%POSS-40%$LiClO_4$ accordingly. But in the spectrum of GPE with IL involved, only one broad peak can be

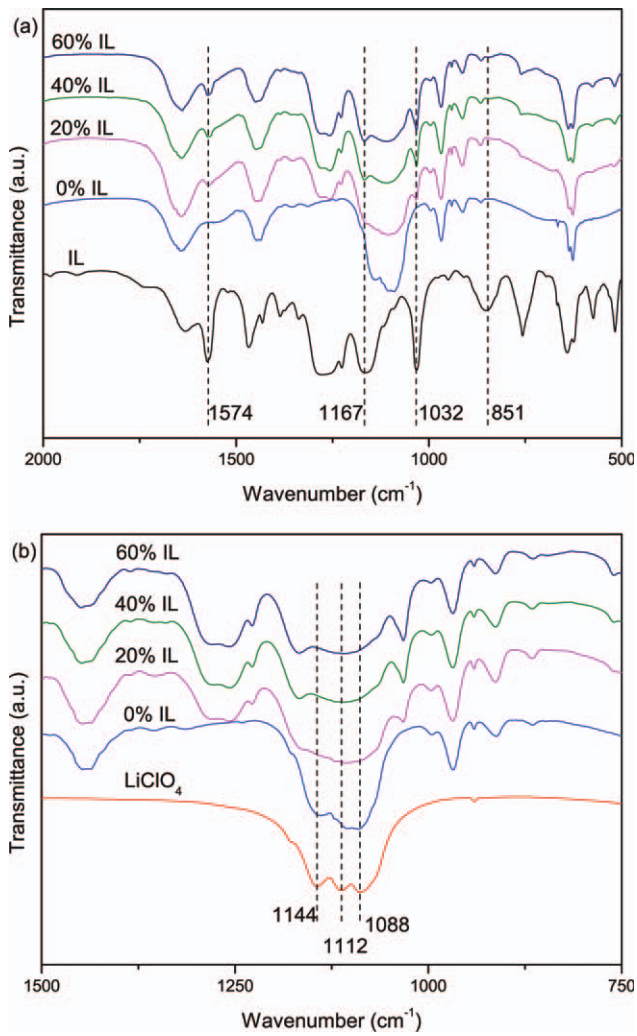

Figure 3 FTIR spectra of $LiClO_4$, IL, and GPE of ATBN-10%POSS-40%$LiClO_4$-*x*%IL. [Color figure can be viewed in the online issue, which is available at wileyonlinelibrary.com.]

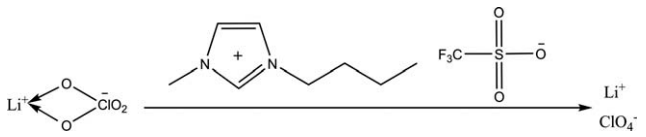

Figure 4 Schematic diagram of the interaction between $LiClO_4$ and BMIMOTf.

observed at 1108 cm^{-1} without branch peaks, which means that the IL molecules weaken the coordination inside $LiClO_4$ and release more free ClO_4^- and Li^+. These variations indicate a particular interaction between $LiClO_4$ and IL, as shown in Figure 4.

FESEM and XRD analysis

The morphology of GPE samples is investigated using FESEM. In the image of ATBN-10%POSS-40%$LiClO_4$-20%IL [Fig. 5(b)], $LiClO_4$ crystals doped in GPE matrix as granular particles can be observed, but in the image of ATBN-10%POSS-40%$LiClO_4$-40%IL [Fig. 5(a)], the homogeneous appearance without $LiClO_4$ crystals detected indicates that $LiClO_4$ salt is totally dissolved, which proves that IL takes effect in improving the dispersion of $LiClO_4$ in GPE system. In the image ATBN-10%POSS-40%$LiClO_4$-20%IL etched by ethanol [Fig. 5(c)], there are plenty of holes caused by the solution of $LiClO_4$ and IL. $LiClO_4$ is mainly dissolved by IL, and the ion transport in the GPE system is mainly owing to the liquid phase including IL and $LiClO_4$, which is one basic characteristic of GPEs.

XRD tests were performed on GPE samples with 10 wt % POSS, 60 wt % $LiClO_4$, and increasing content of IL from 0 to 80 wt %. As shown in Figure 6, the sharp and tense diffraction peaks appearing in the spectrum of ATBN-10%POSS-60%$LiClO_4$ are ascribed to $LiClO_4$ crystals (typically at 21.0, 23.0, and 31.3°), which indicates a high crystallinity of $LiClO_4$ in the composite. Hence, only limited lithium ions are released into GPE matrix making low-charge carrier concentration; besides, the $LiClO_4$ crystals hinder the movement of lithium ions, as a result, low ionic conductivity was shown. As the IL content increasing, the intensity of peaks decreases gradually, which indicates the reduction of $LiClO_4$ crystals. This is caused by the interaction between IL and $LiClO_4$, and such interaction contributes to the dissolution of $LiClO_4$ crystals and releases more Li^+, so accordingly, the ionic conductivity of GPE increases. Moreover, the diffraction peaks owing to $LiClO_4$ crystals almost disappear and only broad low peak corresponding to amorphous polymer is left in the spectrum of the GPE sample with 80 wt % IL when the ionic conductivity of GPE reaches a maximum value.

Ionic conductivity

The ionic conductivity of GPE crosslinked by different content of POSS was measured at 30°C and

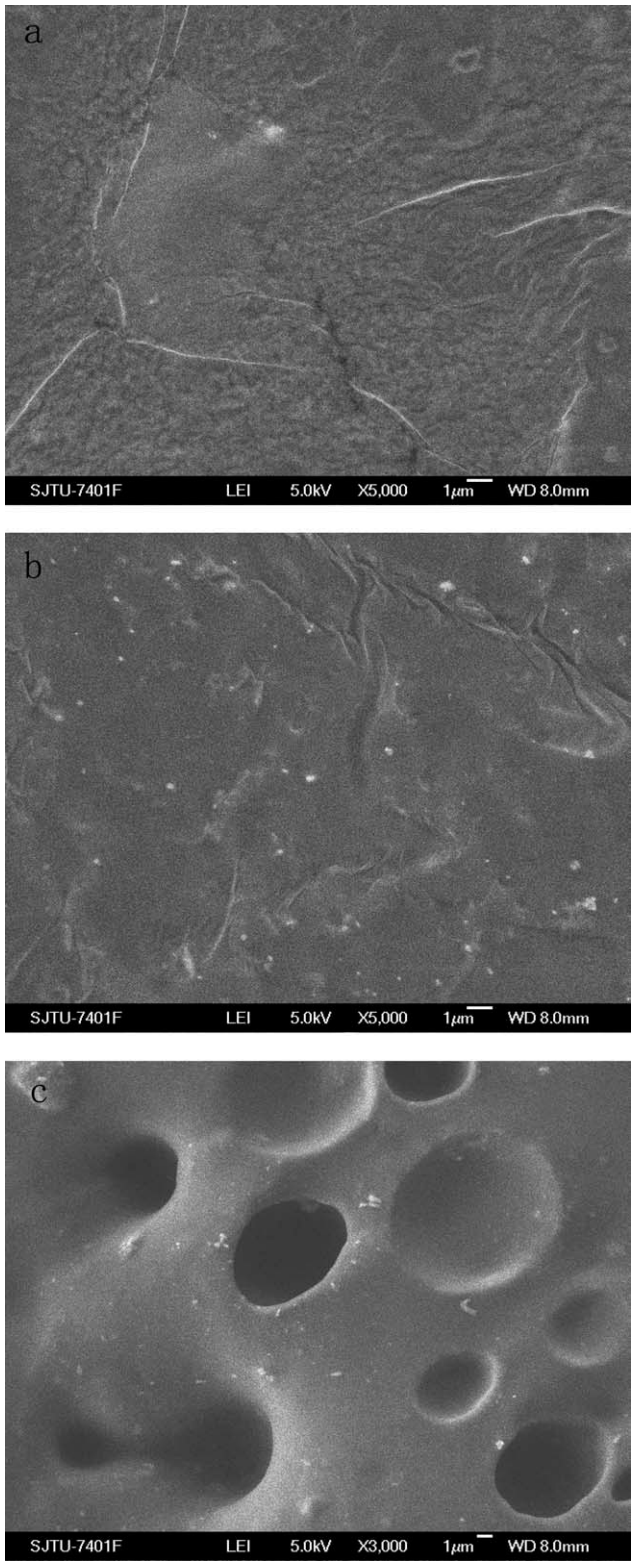

Figure 5 FESEM images of (a) ATBN-10%POSS-40%$LiClO_4$-40%IL without etching, (b, c) ATBN-10%POSS-40%$LiClO_4$-20%IL before and after etching.

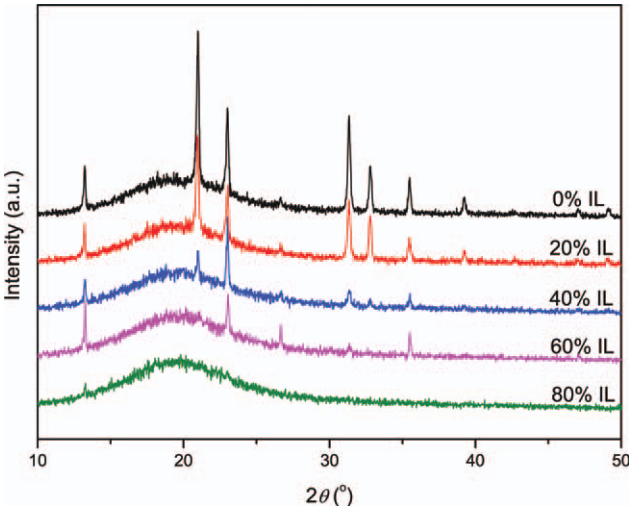

Figure 6 XRD spectra of GPE with 10 wt % POSS, 60 wt % $LiClO_4$, and different IL contents. [Color figure can be viewed in the online issue, which is available at wileyonlinelibrary.com.]

shown in Figure 7. For both GPE with 50 wt % IL, 40 wt % $LiClO_4$, and 50 wt % IL, 60 wt % $LiClO_4$, their ionic conductivity decreases with growth of POSS content. When the content of POSS is 5 wt %, the GPE can exhibit a maximum ionic conductivity of over 10^{-4} S cm^{-1}.

Figure 8 shows the temperature dependence of ionic conductivity for GPE crosslinked by different amounts of POSS. The temperature was varied from 30 to 70°C at a step of 10°C. As expected, the ionic conductivity of all the tested samples increases with the growth of temperature. The relationship between ionic conductivity and temperature for the three GPE samples is well corresponded to Arrhenius-type relationship over the investigated range of temperature. This means that the charge carriers are

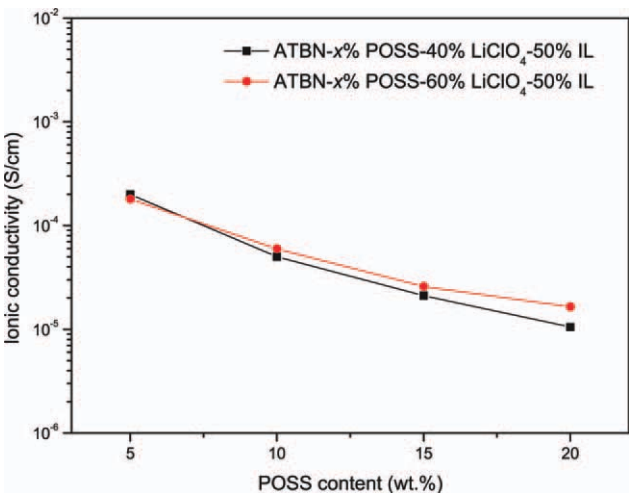

Figure 7 Ionic conductivity of GPE crosslinked by different POSS contents. [Color figure can be viewed in the online issue, which is available at wileyonlinelibrary.com.]

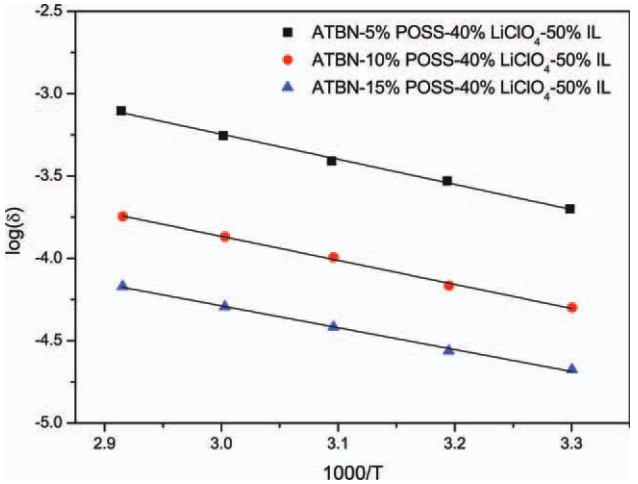

Figure 8 Temperature dependence of ionic conductivity for GPE crosslinked by different POSS contents. [Color figure can be viewed in the online issue, which is available at wileyonlinelibrary.com.]

almost decoupled from the segmental motion of polymer chains and instead coupled with the dynamics of the solvent.[36,37] Activation energy can be estimated from the slope of the three fitted lines. E_a are calculated to be 29.1, 28.0, and 25.5 kJ mol^{-1} for GPE crosslinked by 5, 10, and 15 wt % POSS, respectively. Less POSS leads to less reaction sites for crosslinking, and then less ATBN chains can be attached to POSS with both ends. The free polymer chains are more sensitive to the variation of temperature, and hence the corresponding GPEs show higher activation energy.

Gel content and DMA analysis

As shown in Figure 9, gel content test gives a proof that less POSS content results in lower gel content which indicates lower crosslinking density.

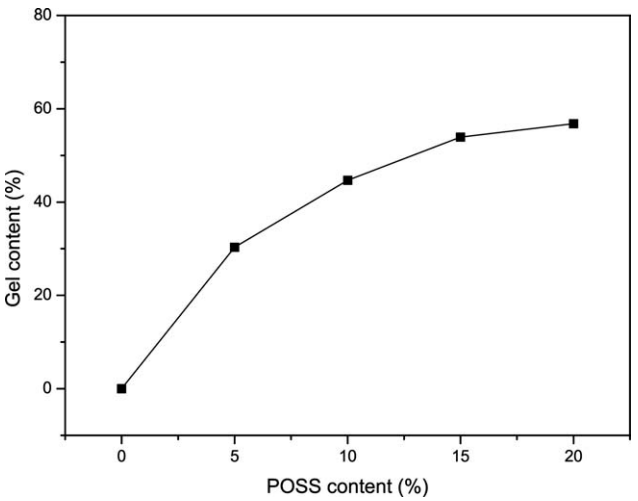

Figure 9 Gel content of GPE crosslinked by different contents of POSS.

Figure 10 shows the storage modulus (G') and loss modulus (G'') of the samples in the frequency range of 0.5–50 Hz measured at 30°C using DMA in tensile mode. GPE crosslinked by higher content of POSS presents relatively higher G' and G'', which is consistent with the results of gel content test. The lower value of G'' compared with G' suggests that the prepared GPEs are elastic because of the crosslinked rubber-like matrix. As epoxy group-functionalized POSS acts as the crosslinking agent in the GPE system, the polymer chains of GPE crosslinked by less POSS are freer and can perform higher mobility, which is helpful in improving ionic conductivity. Lower crosslinking densities give higher ionic conductivities but lower mechanical properties, which means a contradiction between them, and hence to reach the balance is crucial in developing GPEs.

CV analysis

Electrochemical stability of GPE is important for their practical application, because decomposition may cause safety problems and weaken their electrochemical properties. Therefore, CV experiment with Al/GPE/Li cell was carried out to examine the electrochemical stability window, and the CV curve is shown in Figure 11. The test was conducted between −0.5 and 4 V at 25°C. The sample of ATBN-5%POSS-60%$LiClO_4$-50%IL was applied to assemble the cell as electrolytes. The prepared GPE can be stable to about 4 V, meeting the basic requirement of rechargeable lithium batteries. The reversible peaks around 0 V corresponds to lithium plating and stripping of the aluminum electrode.[15] The CV curve indicates high working stability of the cell at room temperature and a potential application for rechargeable lithium batteries.

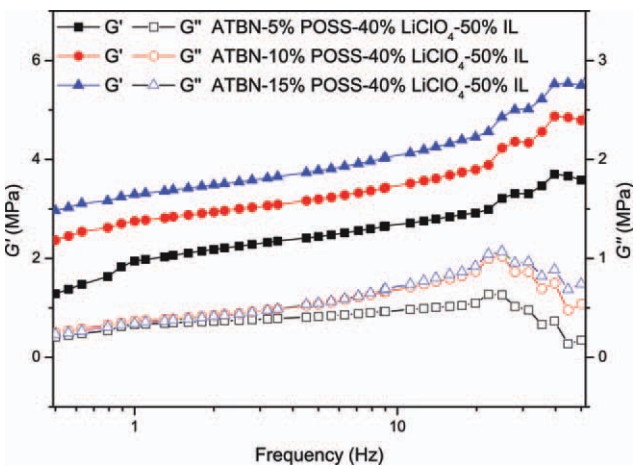

Figure 10 G' and G'' versus frequency for GPE crosslinked by different POSS content etching. [Color figure can be viewed in the online issue, which is available at wileyonlinelibrary.com.]

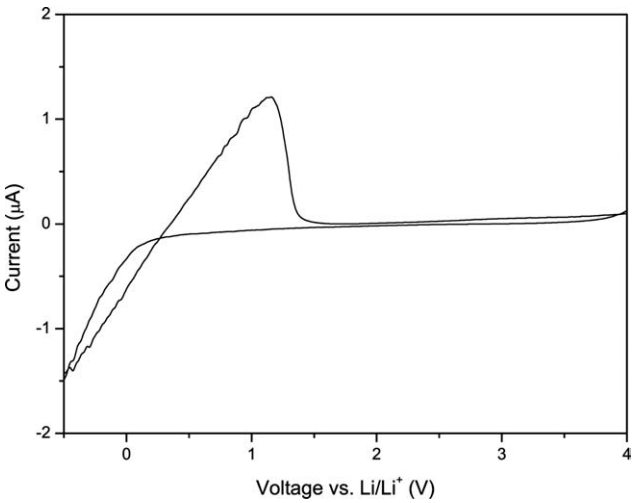

Figure 11 CV curve with Al/GPE/Li cell using ATBN-5%POSS-60%$LiClO_4$-50%IL as electrolytes.

CONCLUSIONS

In summary, GPE based on ATBN was prepared by thermal curing with epoxycyclohexyl POSS as crosslinking agent, $LiClO_4$ as charge carrier, and BMI-MOTf as organic solvent. In GPE system, the interaction between IL and $LiClO_4$ helps to dissolve $LiClO_4$ salt and increases the number of lithium ions, which was proved by FTIR, FESEM, and XRD analysis; therefore, the ionic conductivity increases with the growth of IL content and reaches a peak value. Less content of POSS contributes to higher ionic conductivity but lower gel content and modulus. GPE of ATBN-5%POSS-40%$LiClO_4$-50%IL exhibits a maximum ionic conductivity of 2×10^{-4} S cm^{-1} at 30°C and the temperature dependence of ionic conductivity corresponds to Arrhenius-type relationship ranging from 30 to 70°C. The CV test of the unit cell of Al/GPE/Li indicates that the generated GPE can be stable up to 4 V. The good electrochemical properties make this kind of GPE a promising candidate for rechargeable lithium batteries.

The authors thank Prof. Zhang, Y. M. for the help of measurement, and thank Tang, J. K., Li, J. K., and Gao, P. F. for their intellectual help.

References

1. Feuillade, G.; Perche, P., J Appl Electrochem 1975, 5, 63.
2. Meyer, W. H. Adv Mater 1998, 10, 439.
3. Chen, Z.; Zhang, L.; West, R.; Amine, K. Electrochim Acta 2008, 53, 3262.
4. Sotta, D.; Bernard, J.; Sauvant-Moynot, V. Prog Org Coat 2010, 69, 207.
5. Zhang, Q.; Ren, W.; Yu, H.; Zhang, Y. J Appl Polym Sci 2010, 117, 2340.
6. Song, J.; Wang, Y.; Wan, C. J Power Sources 1999, 77, 183.
7. Stephan, A. M. Eur Polym J 2006, 42, 21.

8. Patel, M.; Bhattacharyya, A. J. Energy Environ Sci 2011, 4, 429.
9. Lee, K. Y.; Chung, W. S.; Jo, N. J. Electrochim Acta 2004, 50, 295.
10. Luo, D.; Li, Y.; Yang, M. J Appl Polym Sci 2011, 120, 2979.
11. Luo, D.; Li, Y.; Li, W.; Yang, M. J Appl Polym Sci 2008, 108, 2095.
12. Liang, W.; Kao, H.; Kuo, P. Macromol Chem Phys 2004, 205, 600.
13. Liang, W. J.; Wu, C. P.; Kuo, P. L. J Polym Sci Polym Phys 2004, 42, 1928.
14. Luo, D.; Li, Y.; Yang, M. Mater Chem Phys 2011, 125, 231.
15. Uchiyama, R.; Kusagawa, K.; Hanai, K.; Imanishi, N.; Hirano, A.; Takeda, Y. Solid State Ionics 2009, 180, 205.
16. Unal, B.; Klein, R. J.; Yocca, K. R.; Hedden, R. C. Polymer 2007, 48, 6077.
17. Galinski, M.; Lewandowski, A.; Stepniak, I., Electrochim Acta 2006, 51, 5567.
18. Armand, M.; Endres, F.; MacFarlane, D. R.; Ohno, H.; Scrosati, B. Nat Mater 2009, 8, 621.
19. Shin, J. H.; Henderson, W. A.; Passerini, S. Electrochem Commun 2003, 5, 1016.
20. Rupp, B.; Schmuck, M.; Balducci, A.; Winter, M.; Kern, W. Eur Polym J 2008, 44, 2986.
21. Marwanta, E.; Mizumo, T.; Nakamura, N.; Ohno, H. Polymer 2005, 46, 3795.
22. Marwanta, E.; Mizumo, T.; Ohno, H. Solid State Ionics 2007, 178, 227.
23. Zhang, Q.; Li, M.; Ren, W.; Zhang, Y. J Macromol Sci B 2011, DOI: 10.1080/00222348.2011.625880.
24. Schwab, J. J.; Lichtenhan, J. D. Appl Organomet Chem 1998, 12, 707.
25. Li, G.; Wang, L.; Ni, H.; Pittman, C. U. J Inorg Organomet Polym 2001, 11, 123.
26. Phillips, S. H.; Haddad, T. S.; Tomczak, S. J., Curr Opin Solid State Mater Sci 2004, 8, 21.
27. Allen, E. C.; Beers, K. J. Polymer 2005, 46, 569.
28. Maitra, P.; Wunder, S. L. Electrochem Solid-State Lett 2004, 7, A88.
29. Zhang, H.; Kulkarni, S.; Wunder, S. L. J Electrochem Soc 2006, 153, A239.
30. Zhang, H.; Kulkarni, S.; Wunder, S. L. J Phys Chem B 2007, 111, 3583.
31. Lee, J. Y.; Lee, Y. M.; Bhattacharya, B.; Nho, Y. C.; Park, J. K. J Solid State Electr 2010, 14, 1445.
32. Liu, Q.; Ren, W.; Zhang, Y. Polym Int 2011, 60, 422.
33. Zhang, L.; Zhang, Q.; Li, J. J Electroanal Chem 2007, 603, 243.
34. Bouchet, R.; Siebert, E. Solid State Ionics 1999, 118, 287.
35. Liang, Y. H.; Hung, C. Y.; Wang, C. C.; Chen, C. Y. J Power Sources 2009, 188, 261.
36. Liang, Y.-H.; Wang, C.-C.; Chen, C.-Y. J Power Sources 2008, 176, 340.
37. Jannasch, P.; Loyens, W. Solid State Ionics 2004, 166, 417.